PARTICLE FLOW MODELING:
TRANSFER CHUTES & OTHER APPLICATIONS

Lawrence K. Nordell

Conveyor Dynamics, Inc. (USA)

1.0   SUMMARY

Modeling of particle or granular behavior using discontinuum mechanics has the potential, today, to be one of the most important scientific advancements to the mining industry. Some particle flow behavior applications are: drilling, blasting, cutting, block caving, digging, scraping, crushing, flow regulating (feeders, transfer chutes, etc.) sliding, vibrating, storing and reclaiming in bins and stockpiles, classifying, segregating, grinding, polishing, coating, floating, and mixing. Investigations range from micro through macro particle mechanics.   The size ranges include molecular interactions through mountainous rock mass dynamics. The particles' working volume is treated like a fabric in which the weave can take many forms, dynamically alter its properties and incorporate single and multiphase behavior. Its thread or particles can rotate, break, slide, dissociate, assume different properties and meander within the weave. One type of fabric is called the Discrete (Distinct) Element Method (DEM). DEM is the term given to the numerical analysis procedure that simulates the behavior within discontinuum mechanics. Particle flow behavior through belt conveyor transfer chutes is given as one elementary example together with its definable benefits. Other DEM applications are highlighted.

2.0   INTRODUCTION

Particle or granular flow modeling is based on the relatively new science of discontinua introduced in geomechanics almost thirty years ago [1]. Its structure is often called a "fabric" referring to the microstructure of the particle mass collection, space between particles within the mass (pore space), arrangement of particles, and their static and dynamic motion interaction contact laws [2]. Loose soils, concrete, and rock with fracture planes are all examples of discrete grain structures forming a discontinuum fabric formation.

Formulation of discontinua by the Discrete (Distinct) Element Method (DEM) was originally developed by Peter Cundall [3], in 1971, and named by him and O. Strack in later 1979 publications [4, 5].

Particle flow modeling is one application of DEM and is the basis of this paper (Ref. Figure 1).

Figure 1 - Large Particles (Ore) on Conveyor Belt

3.0   HISTORICAL PERSPECTIVE

3.1   Continuum Mechanics

Finite Element Method (FEM), Boundary Element Method (BEM), and Finite Difference Method (FDM) have been widely used to study the behavior and design of elastic, visco-elastic and plastic structures under various degrees of deformation, sliding, dilation, and flow. With a few exceptions, these methods require the fabric to be continuous in nature, not allowing for separation, rotation, large scale deformation and displacement. Orthotrophic non-linear laws affecting the fabric may include constitutive variations among the coupled six axis of displacement and rotation. These laws extend to multi-phase media, and in localized elements of the structure. These localized features are difficult to incorporate into continuum models when studying effects such as: buckling, fracture, buoyancy, magnetism, electrostatics, capillary attraction, agglomeration, mixing, cohesion and adhesion.

3.2   Discontinuum Mechanics

Early applications of discontinuum mechanics has centered around rock mechanics (including ice), soil mechanics, flow of fine and large particles, and molecular dynamics [6]. DEM treats particles as an assemblage of individual or distinct bodies. By applying their known individual constitutive properties, contact laws, velocities, displacements, and body forces, their dynamic behavior can be studied over a selected period in time. Physical relationships may extend beyond the phenomenological realm and include phase changes within thermodynamics.

Cundall [8] proposes the term DEM apply only to the class of computer based programs that:

(a)   allow finite displacements and rotations of discrete bodies, including complete detachment between bodies, and

(b)   recognizes new body contacts automatically as the analysis progresses

As the dimension of discontinuum mechanics extends beyond the solid body phase either the definition will need to be expanded or a more general description found. A more appropriate term maybe Multi-Element Method (MEM).

3.2.1 Particle Shapes

In granular/particle flow studies, the formulations have been elementary. Two dimensional studies of circular disks were conducted in the late 1970's and early 1980's. Three dimensional spheres were published in the mid and late 1980's [7, 8, 9]. Higher order shapes are very recent: Two dimensional ellipses in 1992 [10], three dimensional ellipses in 1993 [11] and 1995 [12], two dimensional clustered spheres in 1997 [13], shown in Figure 2a, three dimensional clustered spheres in 1997 [14] shown in Figure 2b, and other types of higher order shapes in 1981 through 1989 [15].

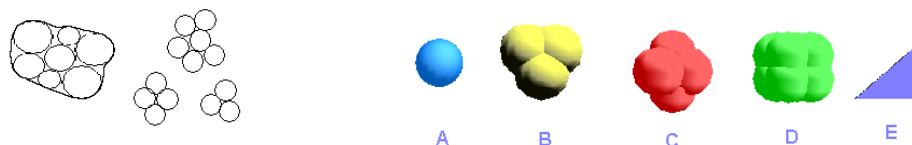Figure 2a - 2-D Clustered Shapes   Figure 2b - Typical 3-D Spherical Cluster
                                                                    Shapes (A-D) & Triangle Surface(E)

Circular disks and mono-spheres are most frequently studied due to the simplified particle contact detecting mathematical algorithms and available computer power.

Much research has been published on the limitations of circular disks and spherical shaped particles. Their shape idealizes particle consolidation and maximizes particle-

rolling action. Most soils and fragmented rock particles are more angular and blocky which: a) increases voids within the fabric of the granular mass, b) increases interlocking between particles, and c) inhibits rolling. Disks and spheres, unlike fragmented particles, produce a low shear resistance and induces rolling that dominates deformation of the fabric. Therefore, disk or spherical shapes do not provide realistic behavior of most mined or processed rock. Furthermore, modeling in two dimensions implies a complete consolidation in the third dimension, which is obviously not possible, thereby altering or skewing the outcome.

Polygonal and hyperquadric shapes have also been studied, but are impractical for large numbered particle models due to the complexity of the contact patterns and large penalty in computational time. Higher order shapes are proposed [15] but still have a large computational time penalty.

Ellipses and clusters of spheres, in proper size distributions and aspect ratios, do provide more realistic particle interlocking and consolidation properties which yield behavior that mimics natural materials [13]. For most real-world problems, 3-D models of non-circular shapes will be required.

3.2.2 Dynamic Equations of Equilibrium

The main governing equations must include for the six degrees of particle motion freedom in 3-D (rectilinear displacement and rotation).

Rectilinear motion, or translational position in the x, y and z planes of an arbitrary element includes acceleration $(\ddot{x}, \ddot{y}, \ddot{z})$, velocity $(\dot{x}, \dot{y}, \dot{z})$, and displacement (x, y, z). For a given element mass (m), contact damping coefficient (c), element elastic non-linear stiffness (k), and applied external force (F), equilibrium is established by the second order differential equation:

$$m\ddot{x} + c\dot{x} + kx - F = 0$$

$$m\ddot{y} + c\dot{y} + ky - F = 0$$

$$m\ddot{z} + c\dot{z} + kz - F = 0$$

Angular momentum of the arbitrary element in equilibrium is governed by Euler's equation: angular acceleration $(\dot{\omega}_1, \dot{\omega}_2, \dot{\omega}_3)$, spin velocity $(\omega_1, \omega_2, \omega_3)$ and external moments (M_1, M_2, M_3), (where the 3-D axes 1,2,3 are the principal normal axes with regards to the element). For the element mass moment of inertia (I_1, I_2, I_3), the Euler equilibrium differential equations about the element's principal normal axes 1, 2, and 3 are:

$$I_1\dot{\omega}_1 + (I_3 - I_2)\omega_3\omega_2 - M_1 = 0$$

$$I_2\dot{\omega}_2 + (I_1 - I_3)\omega_1\omega_3 - M_2 = 0$$

$$I_3\dot{\omega}_3 + (I_2 - I_1)\omega_2\omega_1 - M_3 = 0$$

The method for solving the system of equations follows the finite difference iteration schemes such as found in Walton and Braun [9].

3.2.3 Contact Law and Model Tuning - Solid Phase Flow

Accurate constitutive equations, describing the dynamic particle contact laws between particles and with containment surfaces, are essential for useful model prediction. The

contact laws must relate the distances between particles, interactions of particle structure (i.e. disks and spheres use Hertzian [16] linear elastic solid law), size shape, size, distribution, moisture, elasticity, viscoelasticity, viscoplasticity, and time dependent consolidation and relaxation properties. Disk and sphere shapes are most often used due to the simple test for contact and known surface deformation theory. Contact stiffness between particles must also incorporate both normal and tangential contact relationships with respect to their normal deformation and rotational displacement. Variations of Mindlin's solution given in [17] are often used to describe the non-linear hysteresis of normal and tangential coupled loads [18][19].

Constitutive tuning of particle-to-particle friction, particle-to-wall friction, cohesive forces, adhesive forces, asperite of particles and wall surfaces, moisture and related constitutive properties are well presented in Professor A. W. Roberts tome [20] on bins, chutes, and feeders, et al. Particle-particle and particle-wall yield loci criteria are developed using laboratory direct shear testing of granular material shear and normal stress relationships. The details are outside the scope of this paper. Validation of the DEM model can be accomplished by applying the shear test results into a DEM constructed model to correlate model of shear tester with laboratory measurements. Often field observations are required to fine-tune the models.

4.0 APPLICATIONS IN MINING

A series of applications are presented that illustrate various attributes of solid elastic particle modeling. Four typical uses are presented: 1) Belt conveyor transfer chutes, 2) Coal rilling tower, 3) Belt feeder, and 4) Autogenous grinding mill.

The belt conveyor transfer chute illustrates: 1) particle flow with interlocking between particles, 2) separation and rotation of particles, 3) two types of particle damage that apply to the ore receiving belt at the transfer, and 4) differences in ore flow dynamics between non-cohesive and highly cohesive ores.

A coal rilling tower, belt feeder and autogenous mill are presented as a few further applications without detail on their formulation.

4.1   Belt Conveyor Hard Rock Ore Transfer Chutes

Belt conveyor system can cost tens of millions of dollars. Aside from the mine's ore body life, the conveyor's life expectancy is largely dependent on the life of the belt. Belt life, in high capacity, highly inclined, and hard rock conveyor applications is dependent on the transfer chute design. Typical examples of high cost conveyor applications are illustrated in Figures 3a and 3b.

Figure 3a - 20 km Channar Overland
(2 flights) - Australia

Figure 3b - 15.6 km ZISCO Overland
(1 flight) – Zimbabwe

Figure 4a, b, and c illustrate a typical belt conveyor transfer chute arrangement and flow pattern. Two successful applications, in South Africa and Australia, are given as illustrations of belt conveyor transfer chute modifications using DEM. These installations experienced significant belt damage and frequent belt replacement due to their particle (ore) dynamics.

Substantial improvement was provided by controlling the ore's vertical impact force and slip velocity with the belt's surface by curving the chute's surface.

First, Palabora's primary crushed copper ore (-200 mm) curved chute success is updated from earlier 1994 and 1996 papers [20] [21]. Palabora has a $3 million dollar (NPV) payback over the chute's eight year life. The installation is now almost four years old. It is performing to the predictions.

Second, Robe River's recent primary crushed iron ore (-200 mm) curved chute installation is reviewed. Both Palabora and Robe River illustrate DEM's importance in predicting ore flow dynamics and the different types of damage mechanisms that can be accessed from knowing the particle mechanics behavior.

Figure 5a and 5b show the development of the chute DEM model for particles and boundary constraints. Figure 5a illustrates a transparent side view of the chute. The surfaces of the chute, feeder belt and incline belt are modeled with flat triangulated surfaces. Figure 5b illustrates the non-transparent form. This chute configuration is typical of a hard rock "rockbox" design.

Figure 4a - Transfer Chute Front View

Figure 4b - Transfer Chute & Side View
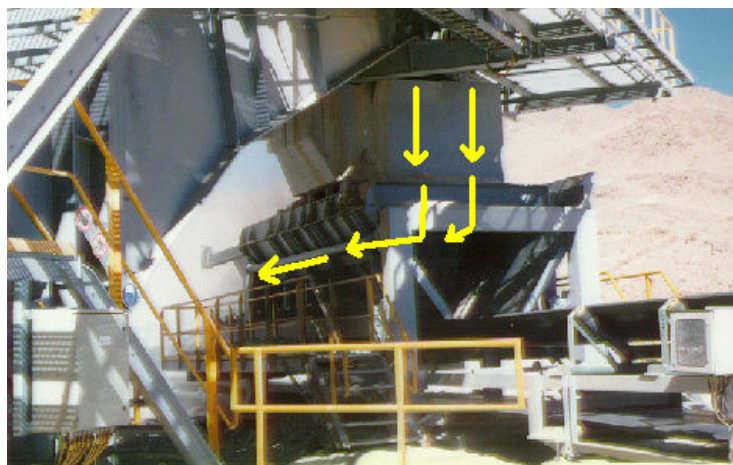
Figure 4c - Transfer Chute & Rear View
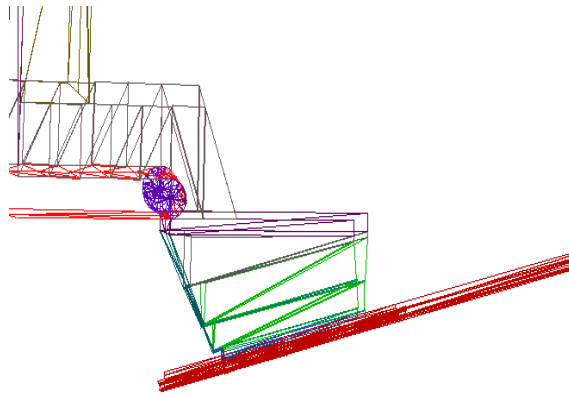
Figure 5a - Chute Containment Surfaces
Transparent View
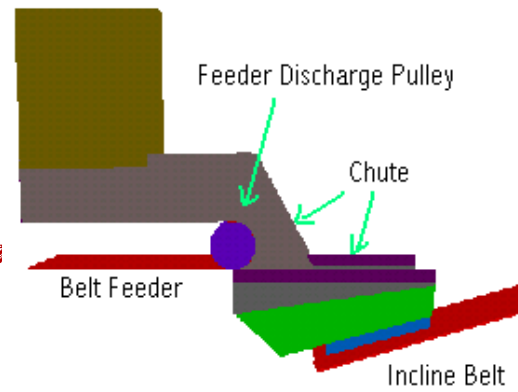
Figure 5b - Chute Containment Surfaces
Solid View

4.1.1 Palabora Rockbox vs. Curved Chute Performance (South Africa)

Palabora experimented with a curved transfer chute, designed by Conveyor Dynamics, Inc. in early 1994, after the initial belt installation wore out in three years. The short life was blamed on the original rockbox chute design. No analytic proof could pinpoint the cause of accelerated wear. Palabora sponsored a study to determine the wear mechanisms and recommendations to improve the rock box design with their 5,000 t/h nominal and 6500 t/h peak flow rates. The original rockbox design flow pattern was analyzed first using a 3-D computational fluid dynamics (CFD) model [21][22]. This CFD model was later updated, in 1996, to the Discrete Element Model (DEM) presented here. The CFD model was difficult to implement and had technical limitations such as rock spillage assessment, rock instability on slopes, particle segregation, and surge irregularities at the beginning and end of ore flow. The CFD model was successful in development of a curved chute configuration for the Palabora installation.

Figure 6a and 6b shows the rockbox general arrangement. Ore is loaded onto the incline belt at a 15.5 degrees slope. The receiving belt has a full speed of 4 m/s. Horizontal ledges are designed to provide rock buildup at the opening to the receiving belt. This creates a static region that the ore flow stream can ride on. The concept minimizes wear and maintenance of the chute's metal surfaces. It also slows down the ore stream forward velocity, in the direction of the receiving belt. This causes a significant increase in ore sliding action (abrasion) on the receiving belt. The 'v' shaped rockbox ledge plate also causes part of the chute's ore stream to be routed along the sides of the ledge and then to be channeled sideways, intercepting the main ore stream at 90 degrees, further decreasing the ore's forward velocity, increasing abrasion damage to the belt.

The ore particle stream, flowing from the crusher ore pocket on and over the feeder conveyor discharge pulley, is captured in the "particle bucket." The "particle bucket" is a velocity vector notation for captured ore particle flow derived from a prior analysis. This allows replaying the discharge stream into various chute configurations under study without the computation penalty of the ore's origins.
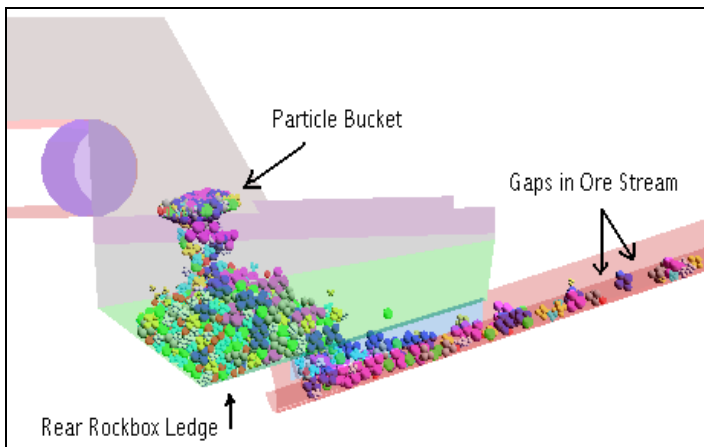
Figure 6a - Palabora Chute Side View
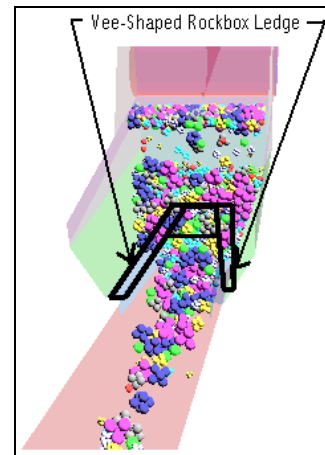Original Rockbox Design
Beginning of Ore Flow Through Chute

Figure 6b - Front View
Original Rockbox Design
Building up Ore Static Bed

Figures 7a and 7b illustrate the ore flow through the curved chute implemented at Palabora. The "particle bucket" discharges the exact ore flow pattern given to the rockbox design. Note, the wider discharge opening onto the receiving belt. The curved chute discharge velocity, along the belt axis, is almost double the rockbox design given by the DEM analysis. Particles are packed and interlock as they flow onto the receiving belt, stopping any rollback.
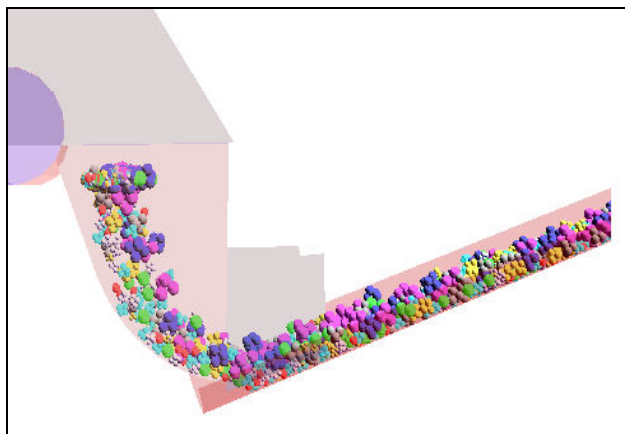
Figure 7a - Curved Chute
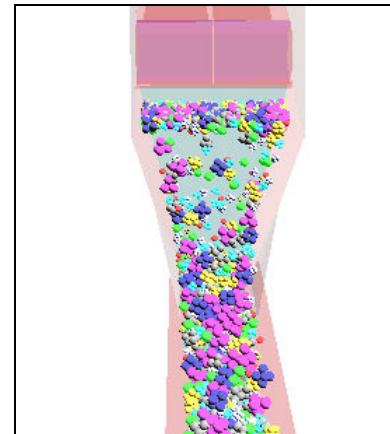
Figure 7b - Curved Chute

Belt damage is divided into two criteria: 1) abrasion (wear) and 2) gouging (tear).

Abrasion is measured by multiplying the applied pressure by the amount of slippage (mPa-m) between rock and belt in direct contact, counting from the point of loading to the end of the sliding region. The abrasion index is divided into a series of small axial strips across the belt's width. The abrasion index is summed for each section of width along the length of the sliding zone.

Gouging is defined as a tearing action. If a rock is sharp enough and has sufficient pressure at the rock tip to exceed the rubber's yield strength, the rubber will crack or tear. The degree of tearing depends on the force and sharpness of the rock, and on the shearing action between rock and belt due to their relative speed differences. Given that the rock sharpness and contact attitude is probabilistic within the ore stream, the only measurable value of certainty is the rock pressure (mPa) and amount of rock slippage on the belt. Therefore, we establish the likelihood or degree of gouging damage from mapping the pressure and slippage field at the loading station across the belt's width in 30-40 discrete width divisions, and along the length in 120-150 divisions. Thus, about 5000 wear and tear points map the attrition zone.

If the specific pressure exceeds a known criterion, then gouging would likely occur. The designer should strive to keep below the gouging threshold. Gouging damage will accelerate belt wear by 3-10 times over simple abrasion.

Comparison of Palabora's rockbox and curved chute wear and tear differences are illustrated in Figures 8 through 11. Figure 10 summarizes wear. Figure 11 summarizes tear.

Figure 8a presents the belt in plan view with the highlighted triangles indicating slippage (abrasion) damage zones for the rockbox. Lighter shades are areas of greater intensity. Figure 8b shows the same effect for the proposed curved chute design.

Figure 8c presents the maximum pressure intensity (gouging and abrasion) of the rockbox, and Figure 8d is the curved chute pressure intensity.

Figure 9a combines pressure and slippage into an abrasion attrition map for the rockbox. Figure 9b shows the comparable abrasion attrition map for the curved chute. The medium dark region at the beginning of the abrasive zone indicate high wear.

Palabora - Differential Velocity (Slippage)
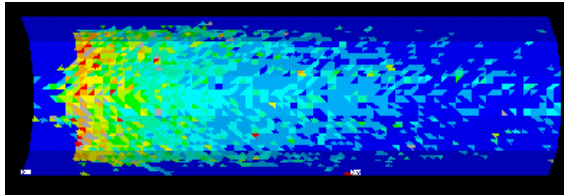
Figure 8a - Rockbox Geometry
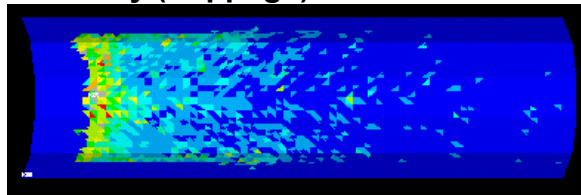
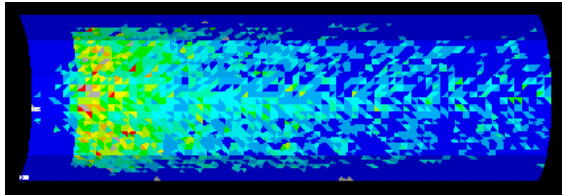Figure 8b - Curved Chute Geometry

Palabora - Maximum Pressure Profile

Figure 8c - Rockbox Geometry

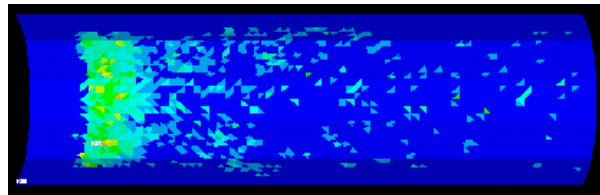Figure 8d - Curved Chute Geometry

High Wear Zone
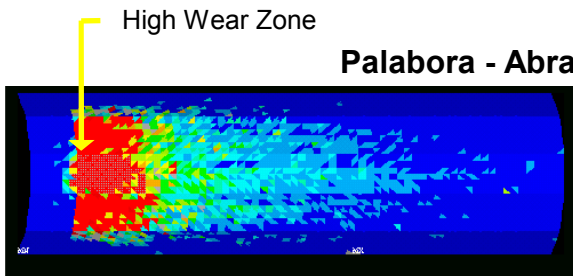
Palabora - Abrasive Wear Profile
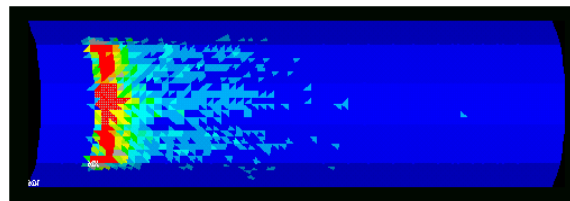

Figure 9a - Rockbox Geometry

Figure 9b - Curved Chute Geometry

From Figure 10, the DEM model predicts the curve chute will improve abrasive wear by a factor of three (3) over the rockbox design. Figure 11 shows that no gouging will take place. These predictions indicate a belt life that should exceed 12 years.

Since the curve chute installation, Palabora has diligently monitored the belt's wear progress every six months over the last 42 months. About 2 mm of belt wear has been measured to date. The belt had an 18 mm top cover. This extrapolates to a 30 year belt life expectancy.

A second load station has been installed this year. The second chute is programmed to load onto the existing main ore stream, thereby protecting the slope belt against impact damage. No analysis has been conducted on the second belt's load influence on belt life.
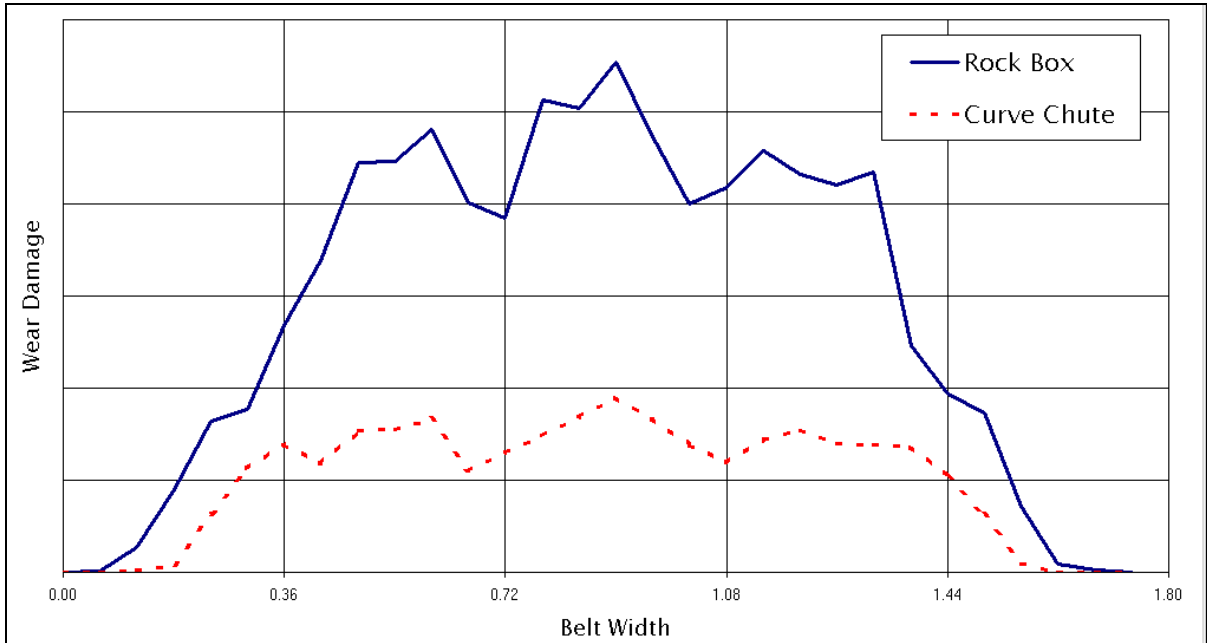
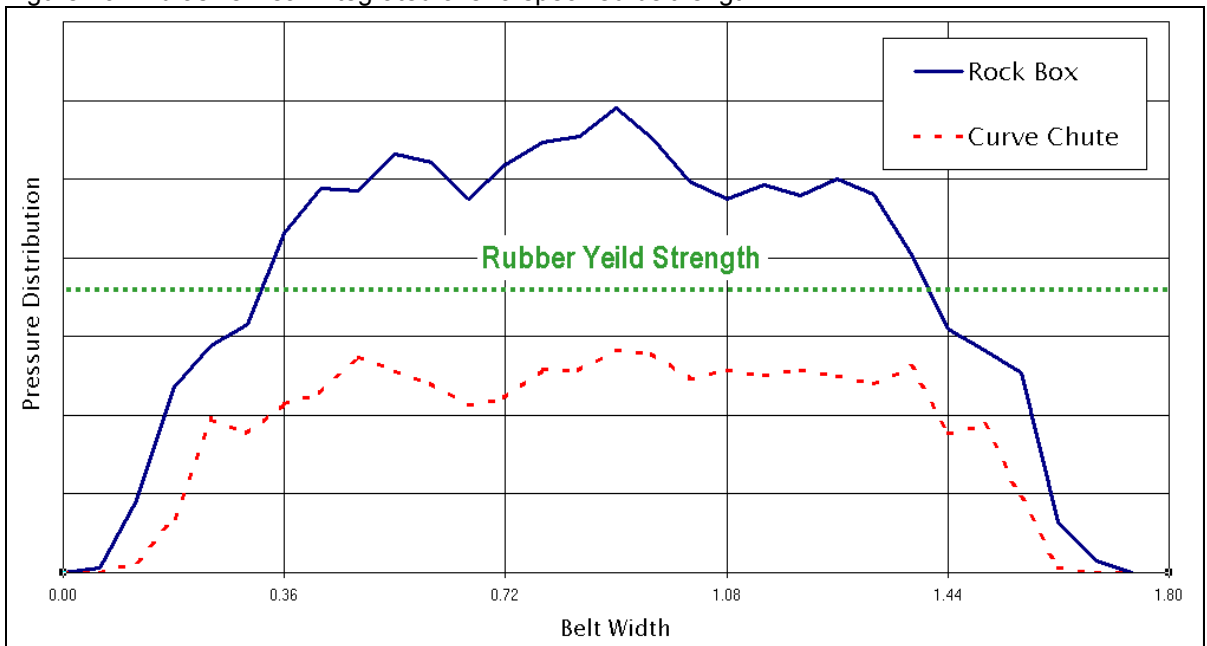Figure 10 - Abrasive wear integrated over a specified belt length

Figure 11 - Maximum pressure integrated over a specified belt length

4.1.2 Robe River Rockbox vs. Curved Chute (Australia)

Robe River commissioned Conveyor Dynamics, Inc. (CDI), in 1995, to improve the design of their primary crushed (-250 mm) iron ore slope belt rockbox. They replace the 12-degree slope belt about every three years due to top cover wear.

The conveyor, which transports up to 6000 t/h, is 1524 mm wide, has a belt velocity of 4 m/s and transports two different types of iron ore. One type is a dry, granular, blocky material that has extremely abrasive properties due to its sharp angular surfaces. The second type is a wet, sticky ore with high fines content, exhibiting strong adhesive and cohesive properties. The wet material can build up on almost vertical surfaces.

Robe River installed a "test" insert, which approximates the CDI recommended curvature, except that the rockbox ledges were not removed. Robe River kept the option of replacing the chute to its original position if the curved insert failed to perform. The test insert has an 8 mm hard facing (600+ Brinnel) welded to a mild steel plate, configured to the required curvature.

Figures 12 and 13 illustrate the plan view of the Robe River belt damage zones based on rock slippage, particle impact pressure, and abrasion index, similar to Palabora.
Figures 12a and 12b show the belt line particle slip velocity versus belt width for the rockbox and curved chute respectively all at the load station.
Figures 12c and 12d show the maximum particle impact pressure across the belt width for rockbox and curved chute respectively.
Figures 13a and 13b show the estimated abrasion wear index between rockbox and curved chute.
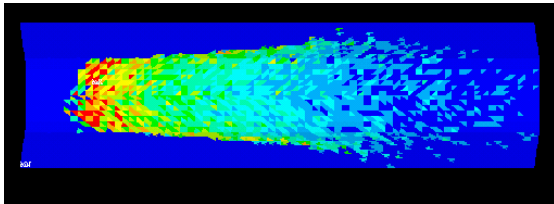
Robe River - Differential Velocity (Slippage)
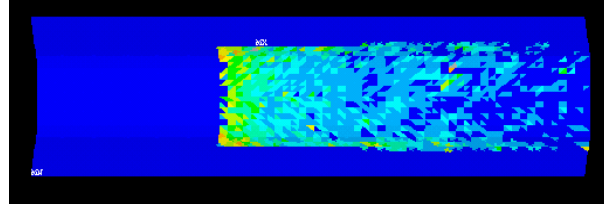

Figure 12a - Rockbox Geometry

Figure 12b - Curved Chute Geometry
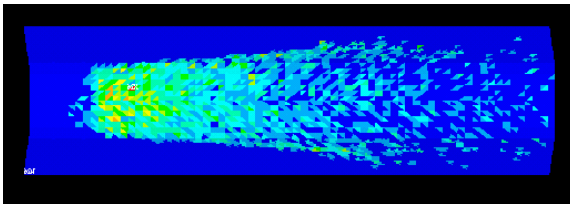
Robe River - Maximum Pressure Profile

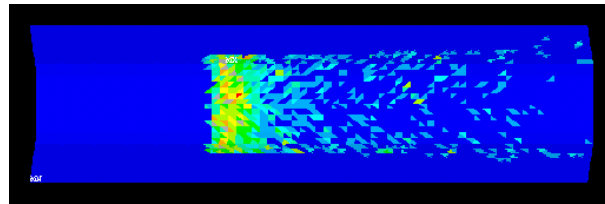Figure 12c - Rockbox Geometry

Figure 12d - Curved Chute Geometry

High Wear Zone

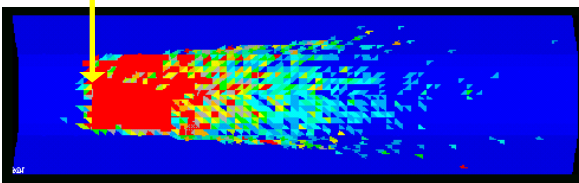## Robe River - Abrasive Wear Profile

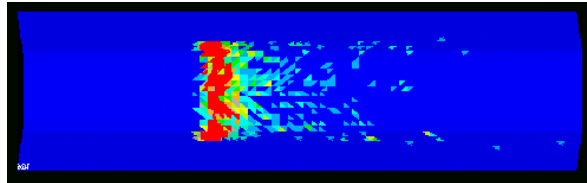

Figure 13a - Rockbox Geometry

Figure 13b - Curved Chute Geometry

Figure 14 summarizes, in graph form, the abrasion index comparison between rockbox and curved chute. Note, the rockbox has a three to four (3-4) times higher wear rate than the curved chute.

Figure 15 summarizes, in graph form, maximum particle impact pressures for the rockbox and curved chute. The curved chute average maximum impact pressure is about 60% of the rockbox. If the pressure reduction brings gouging damage below

the rubber's yield strength, then the belt life will be more than 10 years versus the present 3 years.
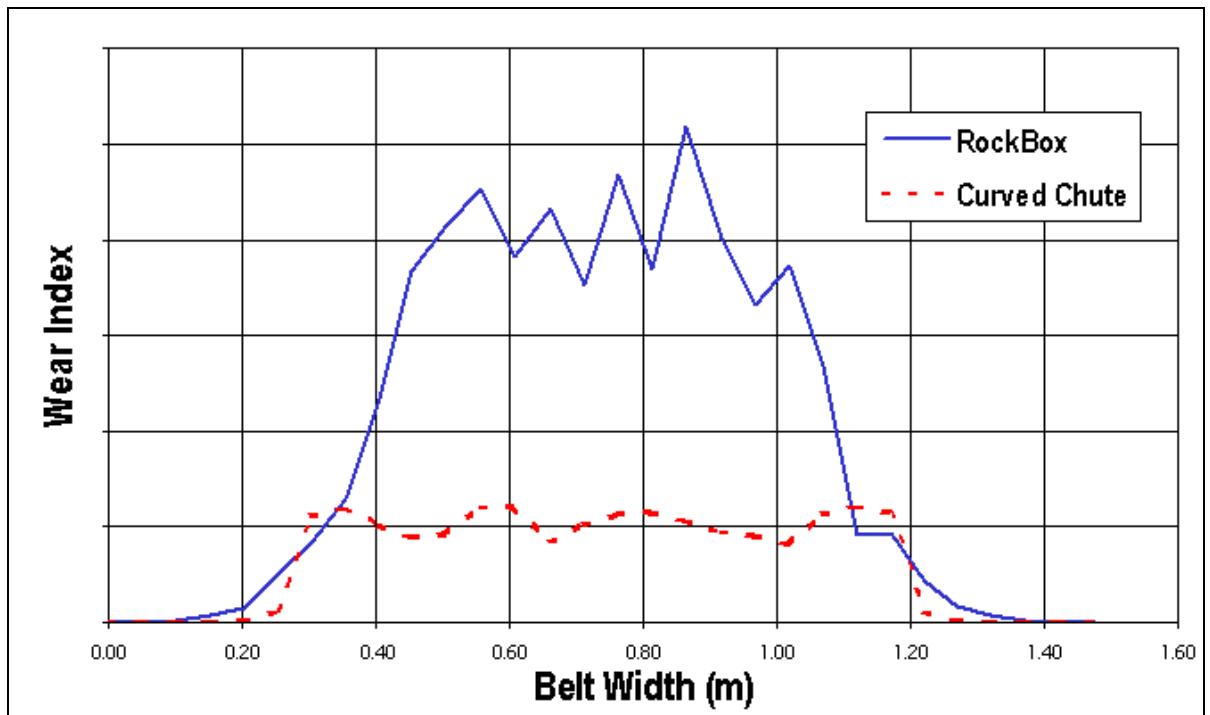

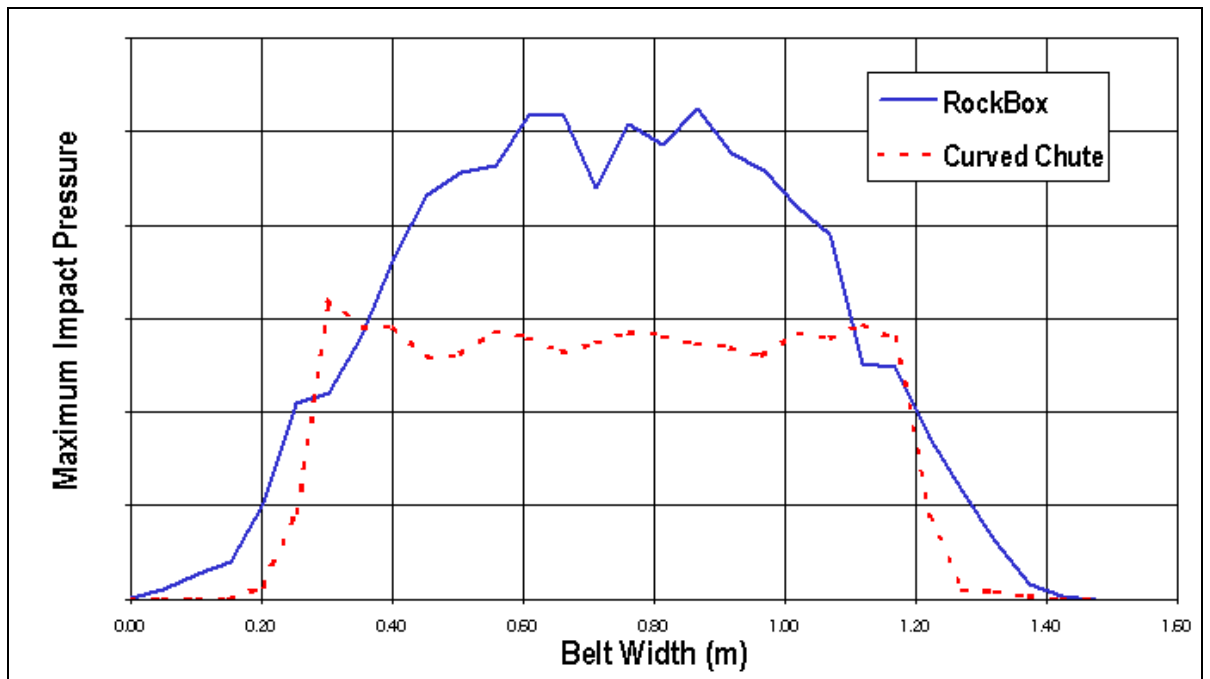Figure 14 - Abrasion (wear) Index vs belt Width - Rockbox vs Curved Chute

Figure 15 - Maximum Impact Pressure vs Belt Width - Rockbox vs Curved Chute

4.2   Belt Feeder Flow Sensitivity

Two examples of belt feeder performance are shown where the same spherical particles are in one case allowed to rotate and in the second case are not allowed to rotate. The latter case simulates particles that have a sticky or cohesive surface. Spherical particles are chosen to illustrate the dynamic range of conditions.

Figure 16 demonstrates, by a series of elapsed time snap shots, the flow behavior of freely rotating (FR) spheres, on the left side versus non-rotating (NR) spheres on the right side for 1 second, 10 seconds, and 18 seconds after the feeder gate is opened.

In the first second, the FR spheres flow over the belt feeder surface and begin discharging into the chute. Particle flow is many times the feeder speed, simulating a fluidized state. The NR spheres, in one second, have moved less than 25% of the distance between feeder gate and the discharge pulley.

After 10 seconds, the FR spheres have emptied 60% of the storage bin. The NR spheres have not yet emptied 45% of the bin.

After 18 seconds, the FR spheres discharge rate is slowing due to loss of hydrostatic head. The NR spheres chute is beginning to plug up. Notice, the flow on the receiving conveyor has stopped and particles have accumulated onto the chute curved surface. These demonstrate the need for proper particle interaction properties.

Figure 16 - Belt Feeder - Spherical Flow With and Without Rotation
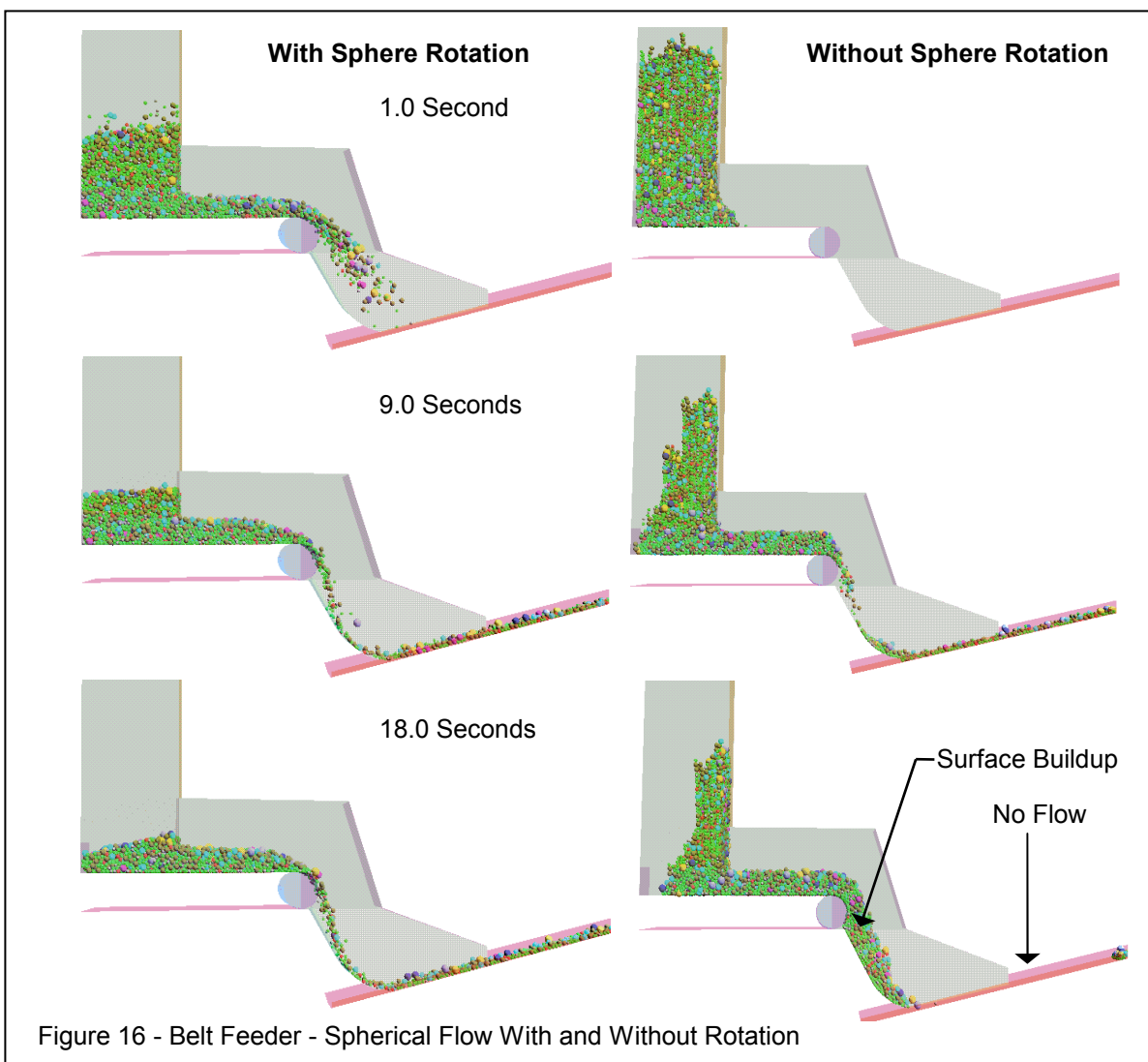
4.3 Rilling Tower Flow

Figure 17 illustrates particle flow down a rilling tower at the initial stage of flow, with the feed hopper at a low ore level, and at the completion of flow with residual material on each bench.
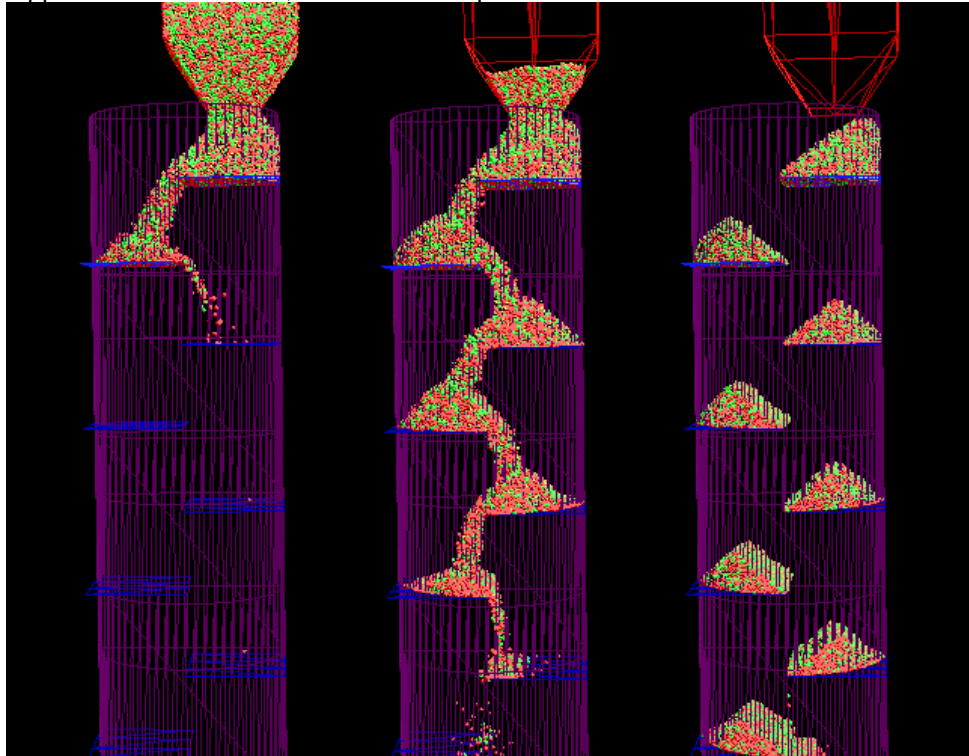

Figure 17 - Rilling Tower Flow - 5 Seconds, 10 Seconds, and 30 Seconds

4.4   Grinding Mill Particle Dynamics

A dry grinding mill, consisting of 60,000 particles, is shown in cross-section. Figure 18 shows a snap shot in time of the approximate steady-state particle flow. Figure 19 illustrates the same flow but taking only 1000 random particles and plotting their instantaneous velocity vectors. This last figure demonstrates the mill's particle vortex pattern, cascade flow, and cataract flow. This shows one area of mill liner damage due to large rock/balls catapulted over the main charge. Many interesting particle and liner attrition and mill power properties can be derived from this model.
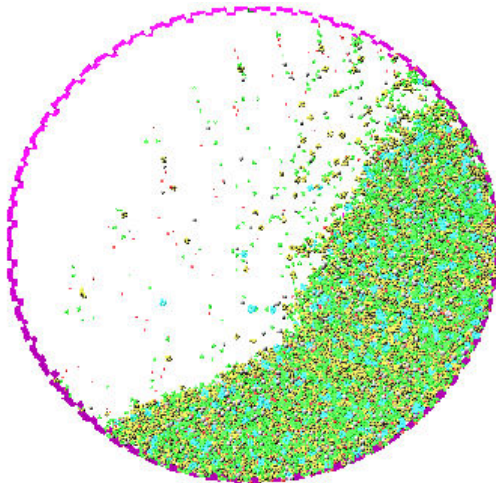

Figure 18 - Grinding Mill Cross Section
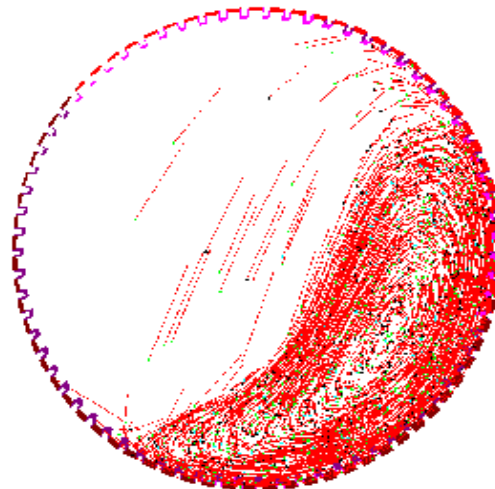Particle Flow Circulation
60,000 Particles

Figure 19 - Grinding Mill Cross Section
Velocity Vector of 1000 Particles

5.0 CONCLUSION

Various applications of DEM particle mechanics have been presented. Their areas of application are as vast as they are varied. We believe this area will contribute significant major benefits to the mining industry in the near future. Efforts are underway to integrate advanced solid large and medium sized granular particle constitutive properties, with fine particle constitutive properties and with fluids. Work has already progressed with gases and granular materials.

The field holds the potential for many more exciting scholarly discoveries as well as commercial benefits to all.

REFERENCES

1.   Goodman, R. E., Taylor, R. L. and Brekke, T. L., "A Model for the Mechanics of Jointed Rock," J. of Soil Mechanics & Foundation Division, Proc. ASCE 94, pg. 637, SM3, 1968.

2.   Mitchell, J. K., "Fundamentals of Soil Behavior, John Wiley & Sons, Inc., 1976.

3.   Cundall, P.A., "A Computer Model for Simulating Progressive Large Scale Movements in Block Rock Systems," Proc. Symp., Int'l Soc. Rock Mechanics, Nancy II, Art. 8, 1971.

4.   Cundall, P. A. and Strack, O. D. L., "The Development of Constitutive Laws for Soils Using Distinct Element Method," Proc. 3rd Numerical Methods in Geomechanics, Aachen, pp. 289-298, 1979.

5.   Cundall, P. A. and Strack, O. D. L., "The Distinct Element Method as a Tool for Research in Granular Media, Part II," Report to NSF, Dept. of Civil and Mineral Engineering, Univ. of Minnesota, 1979.

6.   Evans, D. J. and Murad, S., "Singularity Free Algorithm for Molecule Dynamics Simulations of Rigid Poly-Atomics," Mol. Phys. 42, 6, pp. 1355-1365, 1981.

7.   Strack, O. D. L. and Cundall, P. A., "Fundamental Studies of Fabric in Granular Materials," Interim Report to NSF, CEE-8310729, Dept. of Civil and Mineral Engineering, Univ. of Minnesota, Minneapolis, Minnesota, 1984.

8.   Cundall, P. A., "Computer Simulations of Dense Sphere Assemblies," Micromechanics of Granular Material, Satake and Jenkins, eds., pp 113-123, Elseview Science Publishers, Amsterdam, 1988.

9.   Walton, O. R., Braun, R. L., Mallon, R. G., and Correlli, D. M., "Particle-Dynamics Calculations of Gravity Flows of Inelastic, Frictional Spheres," Micromechanics of Granular Material, Satake and Jenkins, eds., pp 153-161, Elseview Science Publishers, Amsterdam, 1988.

10.   Ng, T. T., "Numerical Simulation of Granular Soil Using Elliptical Particles, Microstructural Characterization in Constitutive Modeling of Metals and Granular Media," The ASME Summer Mech. and Materials Conf., Tempe, Arizona, pp 95-118, 1992.

11.   Lin, X. and Ng, T. T., "Contact Detection Algorithms for Three-Dimensional Ellipsoids in Discrete Element Modeling," Submitted to Int'l J. of Numerical Analytic Methods in Geomechanics, 1993.

12.   Lin, X., "Numerical Study of Granular Soil Behavior Using Random Arrays of Elastic Ellipsoids', Ph.D. dissertation, Univ. of New Mexico, Albuquerque, New Mexico, 1995.

13.   Jensen, R. P., Bosscher, P. J., Plesha, M. E., and Edil, T. C., "DEM Simulation of Granular Media-Structural Interface: Effects of Surface Roughness and Particle Shape," (submitted) Int'l J. of Numerical Analytic Methods in Geomechanics, 1997.

14.   Qiu, X. and Kruse, D., "Design of Conveyor Chute Using Discrete Element Method," Fourth U.S. National Congress on Computational Mechanics (abstract only), San Francisco, California, August 5-8, 1997.

15.   Barr, A., "Superquadrics and Angle-Preserving Transformations," IEEE Computer Graphics and Applications, Vol. 1, pp 1-20, 1981.

16.   Hertz, H., "Uber die Berhrungfester Elastischer korper," J. Renie Angew Math., 92, pp 156-171, 1882.

17.   Mindlin, R. D., " Compliance of Elastic Bodies in Contact," Journal of Applied Mechanics, pp 259-268, September 1949.

18. Seridie, A. and Dobry, R., "An Incremental Elastic-Plastic Model for the Force-Displacement Relation at the Contact Between Elastic Spheres," research Report, Dept. of Civil Engineering, Renssalaer Polytechnic Institute, Troy, N.Y., 1984.

19. Thornton, C. and Randall, C. W., "Applications of Theoretical Contact Mechanics to Solid Particle System Simulations," in Mechanics of Granular Materials, Satake and Jenkins, eds., Elseview Science Publ., Amsterdam, Netherlands, pp. 133-142, 1988.

20. Roberts, A. W., Short Course: "Belt Conveying and Materials Handling - Basic Principles of Bulk Solids Storage, Flow and Handling," TUNRA Bulk Solids Research Associates, September 28-30, 1992.

21. Nordell, L. K., " Palabora Installs Curved Transfer Chute in Hard Rock to Minimize Belt Cover Wear " Bulk Solids Handling, Trans Tech Publications, Vol. 14, No. 4, 1994.

22. Nordell, L. K. and Van Heerden, J. J., "Curved Chutes and Other Improvements at the Palabora Mine " BELTCON 8 conference, RSA, October 1995.